Journal of Alloys and Compounds 509 (2011) 7532–7536

Contents lists available at ScienceDirect

Journal of Alloys and Compounds

journal homepage: www.elsevier.com/locate/jallcom

Impedance analysis of thermally modified $SrBi_2(Nb_{0.5}Ta_{0.5})_2O_9$ ceramics

D. Kajewski*, Z. Ujma

Institute of Physics, University of Silesia, ul. Uniwersytecka 4, 40-007 Katowice, Poland

ARTICLE INFO

Article history:
Received 13 August 2010
Received in revised form 21 April 2011
Accepted 22 April 2011
Available online 29 April 2011

Keywords:
Aurivillius family
Dielectric response
Electrical transport
Ionic conduction
Impedance spectroscopy

ABSTRACT

Aurivillius $SrBi_2(Nb_{0.5}Ta_{0.5})_2O_9$ (SBNT 50/50) ceramics were prepared using the conventional solid-state reaction method. The obtained samples were thermally modified in high vacuum to study the influence of the formed defects on the dielectric and electrical properties of the samples. Scanning electron microscopy with an energy dispersion X-ray spectrometer was applied to investigate the grain structure and stoichiometry of the studied ceramics. Their dielectric properties were determined by impedance spectroscopy measurements. A strong low frequency dielectric dispersion was found to exist in this material which was controlled by thermal modification of the tested ceramics. This phenomenon can be ascribed to the presence of ionized space charge carriers such as oxygen and bismuth vacancies. The dielectric relaxation was defined on the basis of an equivalent circuit. Moreover the temperature dependence of various electrical properties was determined and discussed.

1. Introduction

Aurivillius structured materials, the so-called bismuth layer structured ferroelectrics (BLSFs), have aroused much interest in the recent years due to their potential application in technical devices, e.g. in non-volatile ferroelectric random access memory (FE-RAM). The most promising materials for this particular application are $SrBi_2Ta_2O_9$ (SBT), $SrBi_2Nb_2O_9$ (SBN) and their solid solution $SrBi_2(Nb_{1-x}Ta_x)_2O_9$ (SBNT) since they exhibit fatigue-free properties [1].

The structure of these materials can be described by a general formula $(Bi_2O_2)^{2+}(A_{n-1}B_nO_{2n+1})^{2-}$, where A = Sr, B = Nb or Ta and n is the number of perovskite-like $(A_{n-1}B_nO_{2n+1})^{2-}$ blocks between $(Bi_2O_2)^{2+}$ slabs. In the case of SBNT ceramics $n = 2$ [2]. It is a common feature of some materials from the Aurivillius family, e.g. SBN, SBT and SBNT, in which cation exchange between A-cation in perovskite blocks and Bi in bismuth layers occurs [3–8]. The bigger the ionic radius of A-cation is the stronger the cation exchange becomes [3,4]. Such an exchange in the crystallographic lattice of SBN and SBT may be as high as 1–2%. It leads to inner tensions, distortions and formation of defects such as oxygen vacancies [9,10] and moreover has an impact on electrical properties. Palanduz and Smyth [10] suggest that there exist "rapid pipelines" for oxygen ions in Bi_2O_2 slabs in SBN.

In our previous paper [11] we postulated the existence of easy conduction paths in $SrBi_2(Nb_{0.5}Ta_{0.5})_2O_9$ (SBNT 50/50), on the basis of the results obtained from impedance analysis. We noticed a change in the activation energy of the grain interior dc conductivity in the temperature not related to the para- to ferroelectric state transition. Such a change in the activation energy occurs in the Bi_2O_3–SrO double system and is linked with the structural phase transition from the easy conductive state to the less conductive state when the proper ratio Sr/Bi is obtained [12] and in BIMEVOX family of oxide-ion conductors, derived from a single layered Aurivillius $Bi_4V_2O_{11}$ [13,14]. Therefore we assumed the existence of regions which could be locally treated as the Bi_2O_3–SrO system and which serve as the easy conduction paths in SBNT 50/50 ceramics [11] such as in $SrBi_2Nb_2O_9$ [15].

The aim of the present paper is to determine the influence of defects concentration on the ferroelectric and electric properties of SBNT 50/50 ceramics with the use of the impedance analysis. The concentration of defects was changed and kept under control by thermal treatment of the samples in a highly reductive atmosphere.

2. Experimental procedures

The SBNT 50/50 ceramics, were prepared by a standard mixed-oxide method. The starting raw materials $SrCO_3$, Bi_2O_3, Ta_2O_5 and Nb_2O_5 (all from Aldrich), were weighed and mixed together for 24 h. The mixtures were pressed into pellets and then sintered for 2 h at 950 °C inside a closed double crucible. The obtained substances were crushed, milled in a ball mill and sieved. Such powders were pressed again into pellets and sintered for 2 h at 1150 °C.

All the ceramic pellets were polished to obtain flat and parallel surfaces and for electrical measurements their thickness was of about 0.5 mm. The samples were preheated in a high vacuum (3×10^{-5} mbar) system for 20 min at constant temperature T_h from 350 °C to 900 °C with 50 °C step for composition changes analysis and from 300 °C to 900 °C with 100 °C step for impedance measurements. The samples used for electrical measurements were coated with silver electrodes using a silver paste without thermal treatment.

* Corresponding author. Tel.: +48 32 3591 134; fax: +48 32 2588 431.
E-mail address: dariusz.kajewski@us.edu.pl (D. Kajewski).

0925-8388/$ – see front matter © 2011 Elsevier B.V. All rights reserved.
doi:10.1016/j.jallcom.2011.04.121

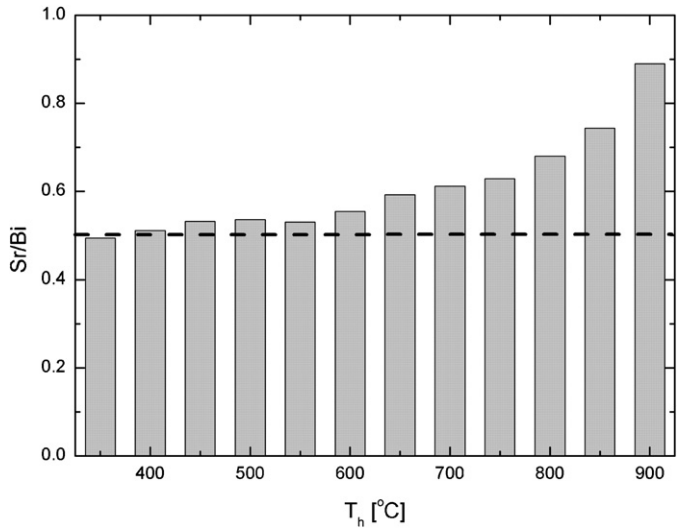

Fig. 1. The variations of strontium to bismuth ratio at chosen preheating temperatures T_h of the samples.

The grain structure and the distribution of all components throughout the grains were examined by a scanning electron microscope (SEM), JSM-5410, with an energy dispersion X-ray spectrometer (EDS) by Oxford Instruments. The investigated ceramics were used for the measurements of the real (G) and imaginary (B) part of admittance (Y^*) as a function of frequency of the measuring field at a constant temperature in the frequency range from 5 Hz to 1 MHz. An automatic measuring system with HP 4192A impedance analyser was used to measure and record G and B.

3. Results and discussion

3.1. EDS composition analysis

The observation of microstructure of SBNT 50/50 ceramics preheated in high vacuum at various T_h did not reveal any change in the microstructure. The EDS analysis, with the implementation of SEMQuant program elaborated by Oxford Instrument, allowed for quantitative microanalysis which indicated no changes in Sr, Ta and Nb concentration with changes of T_h, however a change in Bi concentration was observed. The Sr/Bi ratio changes with T_h are presented in Fig. 1. The nominal Sr/Bi ratio in SBNT 50/50 ceramics is 0.5 and is marked with a dashed line in Fig. 1. As can be seen in Fig. 1, a small excess of Bi was noticed in the investigated ceramics up to T_h = 350 °C. The Sr/Bi ratio closest to the nominal value was achieved at T_h = 400 °C. At T_h range between 450 °C and 550 °C the changes of the ratio were insignificant. Further increase of T_h caused drastic changes of the discussed ratio.

3.2. Dielectric and impedance spectroscopy

Dielectric response of the studied samples was analysed in the same way as in our previous papers [11,15]. The reference sample presented the same character of the dielectric response as the one previously determined for SBNT 50/50 [11]. The presumed existence of a local electrical inhomogeneity of the samples made us decide to use capacitance instead of permittivity to describe the dielectric response of the investigated material.

Capacitance (C) was calculated from the measured imaginary part of admittance from the equation $C = B/\omega$, where ω is the angular frequency. Fig. 2 presents the frequency dispersion of the capacitance of a sample preheated at different temperatures T_h, at the measuring temperatures of 300 °C (Fig. 2a) and 500 °C (Fig. 2b). It is noteworthy that the reference sample exhibits a strong dispersion at low frequencies and it is affected by the temperature change. Such dispersion of C suggests its coupling with the space charge carriers [2,11,14,16]. This behaviour is a common feature of ferroelectrics with a good ionic conductivity [13,14,17–20]. Preheating of the sample at T_h = 300 °C resulted in sudden drop of the dispersion. With the increase of T_h the dispersion became stronger up to T_h = 600 °C. With further increase of T_h the decrease of the dispersion was observed.

As it was mentioned above, the dielectric dispersion is coupled with the space charge carriers forming dipoles and causes a rise in ionic polarisation. The decrease in low frequency dispersion indicates that the number of such dipoles also decreases. This means that more space charge carriers are compensated. As it was mentioned earlier, it is a well known fact that some Bi^{3+} cations exchange Sr^{2+} ions. This leads to the formation of donor centres in perovskite layers and acceptor centres in Bi_2O_2 slabs. Such centres should be self compensating in isotropic structures unlike those in layered structures. Thus acceptor centres in bismuth layers are at least partly compensated by oxygen vacancies whereas donor centres in perovskite layers by electrons or cation vacancies [9,10]. On the basis of these results and those obtained from microanalysis it can be concluded that acceptor centres are most probably responsible for the dielectric dispersion in the reference sample. Thermal treatment in high vacuum led to the formation of additional oxygen vacancies in the sample causing a successive electrical neutralisation of acceptor centres up to T_h = 400 °C. A further increase in T_h led to the increase of the number of oxygen vacancies as well as the rise of the dielectric dispersion. This fact indicates that more unbalanced space charge carriers appeared in the sample. Such behaviour was observed up to T_h = 600 °C and was accompanied by a decrease in Bi content. Further increase of T_h led to the rapid evaporation of Bi cations, which was much faster than that of oxygen anions. This in turn caused the rebalancing of space charge carriers and the decrease of dielectric dispersion.

For a better understanding of the influence of the electric conductivity on the ferroelectric properties, the obtained data were

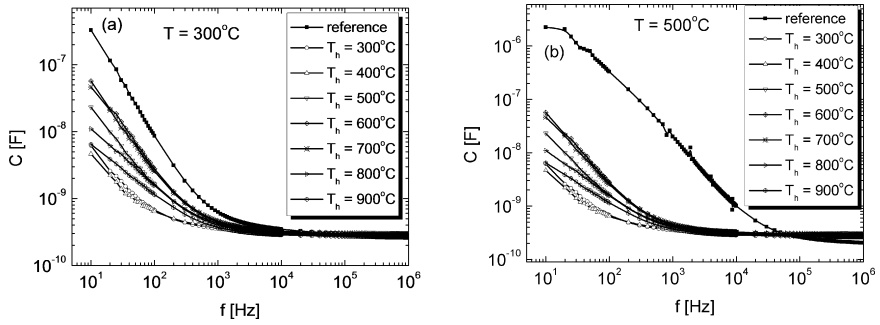

Fig. 2. The variations of capacitance as a function of frequency for chosen preheating temperatures T_h obtained at (a) 300 °C and (b) 500 °C.

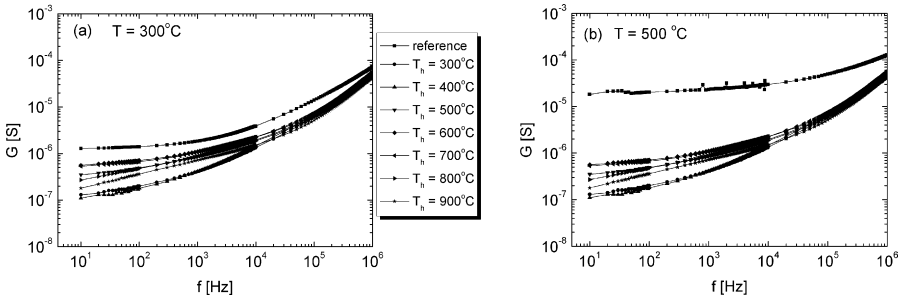

Fig. 3. The variation of real part of admittance as a function of frequency for chosen preheating temperatures T_h obtained at (a) 300 °C and (b) 500 °C.

plotted as a function of frequency to represent a variation of the real part of admittance (G) (Fig. 3). One can notice that the plateau of conductivity, i.e. frequency independent values of conductivity corresponding to the dc conductivity, is clearly visible in the low frequency region for the reference sample. The frequency range where it can be observed changes with T_h. In the higher frequency region a strong dispersion of electric conductivity can be seen. The changes of $G(f)$ in this region can be described as proportional to f^n, where f is the frequency and n is the parameter depending on both the measuring temperature and T_h. The character of these changes does not depend on the measuring temperature.

To find the proper electrical equivalent circuit, the obtained data were presented by applying the impedance (Z^*) formalism (Fig. 4). The obtained curves were neither semicircles nor circular arcs. In the high frequency region the Debye behaviour was observed where the angle between the tangent of the arc and the real axis was 90°. Whereas in the part of the arc where $f \to 0$ the angle was less than 90° and was temperature dependent. It is noteworthy that with the preheating of the sample at T_h = 300 °C both Z' and Z'' drastically increased in comparison with the reference sample, especially at high temperature (Fig. 4b). The increase of T_h to 400 °C led to the increase of the real and the decrease of the imaginary part of the impedance. For T_h = 500 °C and 600 °C the decrease of Z' and the increase of Z'' occurred. With further increase of T_h the increase of Z' and the decrease of Z'' was again observed.

On the basis of the above observations and our previous papers [11,15] an equivalent electrical circuit shown in the inset to Fig. 4a was proposed, where CPE stands for a constant phase element. The equivalent circuit for this ceramics consists of two branches in the series. The first represents intragranular properties and takes into account the dielectric and impedance relaxation and the second corresponds to the grain boundary effects where R_{gb} and CPE_{gb} are parallel. The complex impedance in this model is expressed by the equation:

$$Z^*(\omega) = Z_g^* + Z_{gb}^* \tag{1}$$

where

$$Z_g^* = \frac{R_g}{1 + C_g R_g j\omega + A_0 R_g (j\omega)^n} \tag{2}$$

describes intragranular properties, and

$$Z_{gb}^* = \frac{R_{gb}}{1 + B_0 R_{gb} (j\omega)^m} \tag{3}$$

represents the grain boundary effects. A_0, B_0, n and m are the temperature dependent parameters. To calculate all the parameters fitting was performed using the complex nonlinear least-squares fitting [21] of both real and imaginary parts of complex impedance (Eqs. (1–3)).

This procedure revealed that in the temperature from 365 °C to 425 °C only Z_g^* is of significant importance. This temperature varied with no correlation to T_h. The calculated parameters R_{gb}, B_0, m, varied in the following ranges: 30–90 kΩ, 4.5×10^{-6} to 2.0×10^{-9} s^m Ω^{-1}, 0.53–1.0, respectively for T_h 300–900 °C.

From Eq. (2) it was possible to calculate the dc conductivity of grains $G_{dc} = R_g^{-1}$. It can be seen in Fig. 5 that in the low temperature region the conductivity rises with the increase of T_h up to T_h = 600 °C. Further increase of T_h causes a slight decrease in conductivity. At the high temperature region conductivity continues to decrease with the increase of T_h. Furthermore the temperature changes of the grain dc conductivity for all T_h temperatures cannot be described by one activation process only. As in the case of our reference sample temperature of the grain dc conductivity mechanism change is not associated with the phase transition temperature (T_C = 340.6 °C [2,11]).

The calculated capacity of the grains C_g indicates a high frequency dielectric response of the sample. The values of capacity C_g for different T_h as a function of temperature is presented in Fig. 6. This characteristic shows the typical maximum, correlated with the phase transitions from the ferro- to paraelectric state. One can notice that up to T_h = 600 °C the capacity exhibits only a small increase with the rise of T_h. The increase of T_h to 700 °C causes a

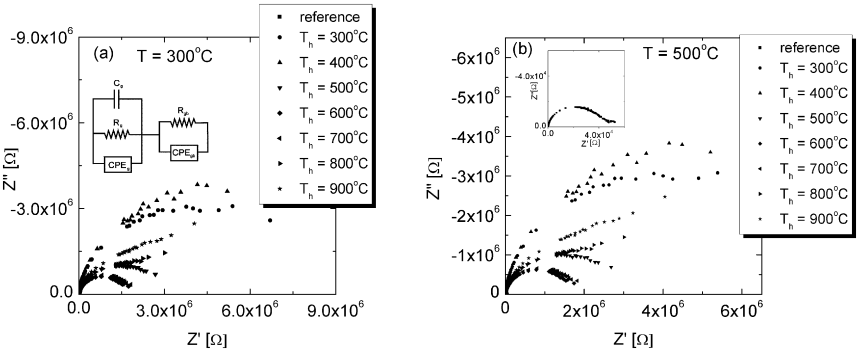

Fig. 4. Complex impedance plots for chosen preheating temperatures obtained at (a) 300 °C and (b) 500 °C, the equivalent circuit (inset in Fig. 1a) and the complex impedance plot for reference sample obtained at 500 °C (inset in Fig. 1b).

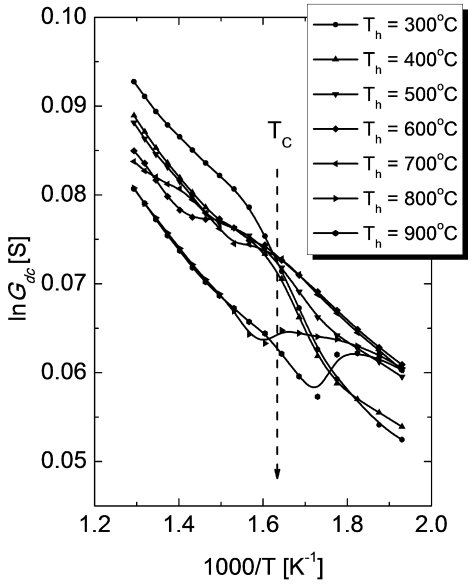

Fig. 5. Arrhenius plot of bulk (dc) conductance for chosen preheating temperatures.

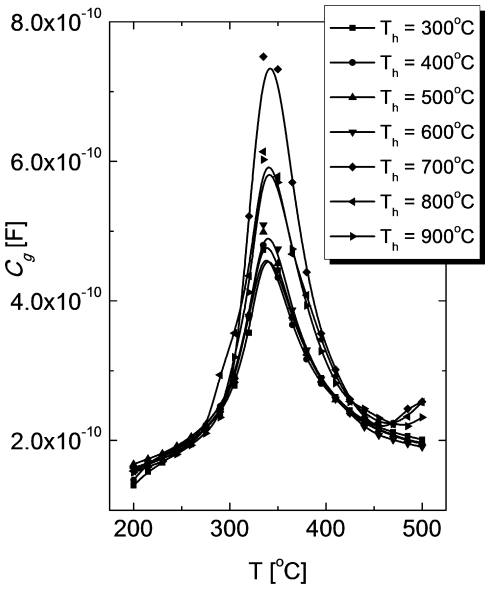

Fig. 6. The temperature dependence of high frequency grains capacitance for chosen preheating temperatures.

rapid increase of C_g, especially in the T_C region. Further increase of T_h leads to a decrease in C_g. It can be clearly seen that for T_h over 600 °C, in the high temperature region, a small increase of C_g with the increase of temperature occurs. Such an effect can be caused by the high electronic conductivity which cannot be neglected at the measuring electric field when its frequency is only up to 1 MHz.

The changes of n with temperature characterize the coupling between charge carriers taking part in the polarization process (the lower the n value the stronger the ion-ion coupling [22]). The n parameter values were the highest for T_h = 300 °C and 400 °C between 0.65 and 0.45 for low and high measuring temperatures, respectively. For temperatures T_h over 400 °C the parameter revealed a local anomaly (a local minimum), whose temperature changes with T_h. This temperature is the same as the temperature at which the local anomaly of the grain dc conductivity occurred (Fig. 5). For this range of T_h the values of n varied from 0.2 to about 0.5.

The A_0 parameter from Eq. (2) describes the contribution of the mechanism linking the universal Jonscher law to polarizibility and, together with parameter n, provides information about the source and the strength of the low frequency dispersion. Owing to the complex capacity $C^* = 1/(j\omega Z^*)$ and Eq. (2) it was possible to describe the total grain capacity C, by the following equation:

$$C = C_g + A_0(T)\sin\left(\frac{n(T)\cdot\pi}{2}\right)\cdot\omega^{n(T)-1} \quad (4)$$

where C_g is the calculated high frequency capacity and the second part of the equation describes the contribution to capacity from space charge carriers (C_{charge}).

This part of Eq. (4) allowed us to describe C_{charge} both as a function of frequency and temperature. This is illustrated in Fig. 7a for different T_h and a chosen driving frequency (100 kHz) of the measuring electric field. One can notice that already at this relatively high frequency the contribution of space charge carriers should not be neglected. Especially that the second anomaly is observed in the temperature range above T_C. It moves towards T_C with the increase of T_h and gives rise to total capacity C. Moreover it is also noteworthy that with the increase of T_h the contribution of C_{charge} to the total capacity decreases at this frequency. The temperature dependence of C_{charge} for T_h = 600 °C at various frequencies of the measuring field is presented in Fig. 7b. For a better insight into the influence of driving frequency on C_{charge} we plotted the $C_{charge}(T)$ dependency

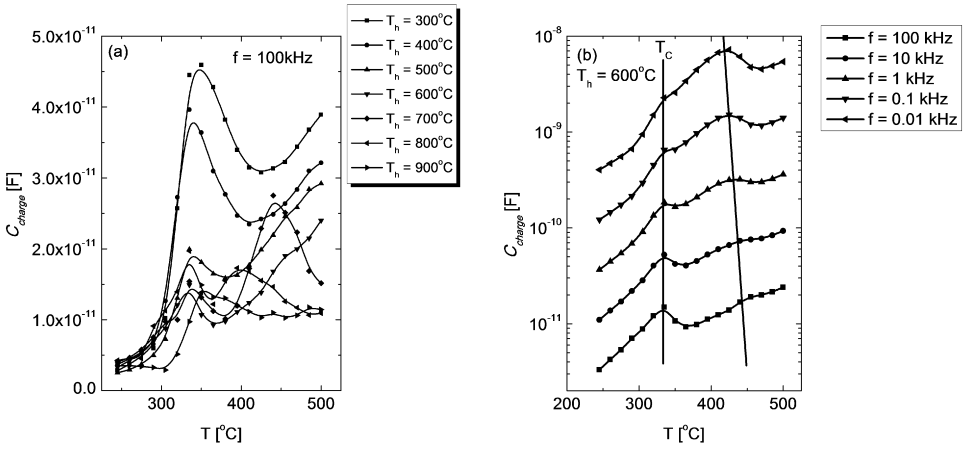

Fig. 7. The temperature dependence of charge carrier-induced capacitate for (a) driving field frequency 100 kHz for chosen preheating temperatures and (b) for preheating temperature 600 °C for chosen frequencies of the measuring field.

in the log scale. It can be seen that with the increase of frequency the C_{charge} contribution decreases and the second anomaly moves towards higher temperatures.

The presented analysis of the electric and dielectric properties of the thermally modified ceramic samples of SBNT 50/50 allowed us to determine the equivalent electrical circuit and to present the possible reason of the sudden change both in the impedance value as well as in the activation energy of electric dc conductivity in grains. By changing bismuth and oxygen concentration we were able to control conductivity in the studied ceramics. It is noteworthy that in the low temperature region the dc conductivity of grains increased with increase of T_h – this remains in agreement with logical predictions. The appearance of Bi and O vacancies increases electrical conductivity of the grains. However in the high temperature region electrical conductivity decreases with the increase of T_h. Moreover the temperature, at which the change of grain conductivity occurs, changes with T_h, i.e. both with the Bi/Sr ratio and the number of oxygen vacancies. Such behaviour is only possible when Bi_2O_2 slabs with incorporated strontium cations are treated locally as a double Bi_2O_3–SrO system, as postulated in our previous papers [11,15]. This would explain the sudden drop in electric conductivity of grains in a certain temperature range, i.e. the easy conduction paths enable rapid oxidation of the grain interiors and hence lead to the neutralization of space charge carriers.

4. Conclusions

Dielectric and impedance behaviour of thermally modified SBNT 50/50 ceramics was investigated over a wide temperature and frequency range. The controlled changes of defect concentration allowed for a better insight into the mechanism of oxygen diffusion in these materials as well as into the problem of low frequency dielectric dispersion. Moreover the performed impedance spectroscopy studies enabled us to justify the application of the postulated equivalent electrical circuit. The changes of oxygen defect concentration and Sr/Bi ratio led to strong changes in the electrical conductivity of the grain interior and were linked with a thermally activated motion of ionised oxygen vacancies. Only a high defect concentration resulted in changes of the ferroelectric properties such as capacity of grains in the vicinity of the ferroelectric phase transition. Thus we assume that regions with an adequate Sr/Bi ratio are responsible for the electric properties of SBNT 50/50 ceramics and furthermore act as easy conduction paths. It is noteworthy that only perovskite layers stimulate ferroelectric properties whereas defect concentration, i.e. space charge carriers, is responsible for the existence of the low frequency dielectric dispersion. To determine whether Bi_2O_2 layers with the incorporated Sr cations act as easy conductive paths or whether the volume of the sample with an adequate proper Sr/Bi exchange ratio plays such a role, it is necessary to conduct further studies in this field. However on the basis of the local conductivity measurements in $SrBi_2Nb_2O_9$ ceramic samples [13] one can predict that rather the volume of the sample is responsible for creation of the easy conductive paths. Most probably, as in the case of BIMEVOX family, the change in the activation energy of the dc conductivity is related to the structural phase transition causing ordering and disordering of the oxygen vacancies in the double SrO–Bi_2O_2 system [13,14] i.e. in local easy conductive paths.

References

[1] C. A-Paz de Araujo, J.D. Cuchlaro, L.D. McMillan, M.C. Scott, J.F. Scott, Nature 374 (1995) 627–629.
[2] D. Kajewski, Z. Ujma, K. Szot, M. Pawełczyk, Ceram. Int. 35 (2009) 2351–2355.
[3] S.M. Blake, M.J. Falconer, M. McCreedy, P. Lightfoot, J. Mater. Chem. 7 (1997) 1609–1610.
[4] R. Macquart, B.J. Kennedy, Y. Shimakawa, J. Solid State Chem. 160 (2001) 174–177.
[5] C.H. Hervoches, P. Lightfoot, J. Solid State Chem. 153 (2000) 66–73.
[6] B.J. Kennedy, Ismunandar, J. Mater. Chem. 9 (1999) 541–544.
[7] C.H. Hervoches, A. Snedden, R. Riggs, S.H. Kilcoyne, P. Manuel, P. Ligthfoot, J. Solid State Chem. 164 (2002) 280–291.
[8] Q. Zhou, B.J. Kennedy, M.M. Elcombe, J. Solid State Chem. 179 (2006) 3744–3750.
[9] A.C Palanduz, D.M. Smyth, J. Electroceram. 5 (2000) 21–30.
[10] A.C. Palanduz, D.M. Smyth, J. Electroceram. 11 (2003) 191–206.
[11] D. Kajewski, Z. Ujma, J. Phys. Chem. Solids 71 (2010) 24–29.
[12] N.M. Sammes, G.A. Tompsett, H. Naefe, F. Aldinger, J. Eur. Ceram. Soc. 19 (1999) 1801–1826.
[13] S. Bega, A. Al-Alasa, N.A.S. Al-Areqib, J. Alloys Compd. 504 (2010) 413–419.
[14] Y. Taninouchia, T. Udab, T. Ichitsubob, Y. Awakurab, E. Matsubarab, J. Alloys Compd. 509 (2011) 5833–5838.
[15] D. Kajewski, Z. Ujma, Phase Transitions 83 (2010) 897–908.
[16] D. Dhak, P. Dhak, P. Pramanik, Appl. Surf. Sci. 254 (2008) 3078–3092.
[17] A.K. Jonscher, Philos. Mag. B 38 (1978) 587–601.
[18] A.K. Jonscher, D.C. Dube, Ferroelectrics 17 (1977) 533–536.
[19] Z. Lu, J.P. Bonnet, J. Ravez, P. Hagenmuller, Solid State Ionics 57 (1992) 235–244.
[20] T.A. Nealon, Ferroelectrics 76 (1987) 377–382.
[21] B.A. Boukamp, J. Electrochem. Soc. 142 (1995) 1885–1894.
[22] K.S. Rao, D.M. Prasad, P.M. Krishna, B.H. Bindu, K. Suneetha, J. Mater. Sci. 42 (2007) 7363–7374.